

Solar-B EIS * EUV Imaging Spectrometer	Further investigations into radiation shielding - simulations using SPENVIS
--	--

Title	Further investigations into radiation shielding - simulations using SPENVIS
Doc ID	EIS-CCD-desnote-005
ver	1.0
Author	Chris McFee
Date	23 September 1999

Introduction

The potential radiation dose for the Solar-B EIS CCDs was discussed in reference [1], and the potential effect of that radiation dose was discussed in reference [2]. Whilst the effect of ionising radiation on CCD areas such as flat band voltage shifts was not a cause for concern (although the transient effects on image quality may be) there was a potential problem with the effect of Non-Ionising Radiation damage on the CCD's Charge Transfer Inefficiency (CTI). Consequently, it was recommended that an operating temperature of around -80°C or so may be necessary to ensure adequate CTI. However, subsequent thermal studies have shown that such a low temperature may be difficult to reach.

It should be noted that the degree to which there could be a CTI is not yet known. The above studies have indicated that there is a potential problem, and measurements are planned on representative CCDs to see how the CTI changes after known radiation doses.

However, for the purposes of this study, it has been assumed that there is a CTI problem and that there are several ways by which adequate CTI can be achieved:

1. use active cooling to reach the suggested temperature;
2. improve the radiation shielding around the device to reduce the overall radiation dose and hence the likely damage and CTI degradation.

It should be noted that option (2) would also have the effect of reducing any transient image problems caused by incident radiation. Option (1) will be investigated elsewhere, and option (2) will be discussed in this memo.

To investigate the potential improvements in CTI that could be obtained using additional shielding, the ESA collection of programs called "SPENVIS" was used to calculate the variation in particle flux and

ionising radiation dose with shielding thickness. In addition to using the results from SPENVIS to estimate the potential improvement to CTI, the results were also used to predict the potential improvement in a number of CCD parameters: dark signal; flat band voltage shifts due to ionising radiation; and transient image events.

The calculation of total dose using SPENVIS

To calculate the potential effect of differing amounts of shielding, the ESA environmental models (known as "SPENVIS") were used. Use of these models is freely available on the web ¹. The procedure for calculating the total ionising dose and the total proton dose described below.

1 Calculate the orbital parameters

The parameters used for Solar-B were:

- Orbital inclination - 98°
- Mean orbital height - 600km.
- Initial ascending node - 0 hours
- Initial starting date - 1 August 2004

The program will calculate the orbital profile of Solar-B for the subsequent twenty orbits. However, one of the most important sources of radiation is the South Atlantic Anomaly (SAA) and the extent to which the spacecraft orbit calculations for twenty passes will go through the SAA depends upon the initial ascending node. Consequently, calculations were performed for a number of differing ascending nodes, and the ionising radiation dose and proton dose were averaged from these calculations. The values used were: 0 hours; 5 hours; 8 hours; 11 hours and 14 hours.

2 Calculate the trapped proton dose

These values were automatically calculated AP8-MIN (for protons) and AE8-MIN (for electrons) for one year's duration. If the trapped proton dose is required near Solar maximum, then AP8-MAX and AE8-MIN can be used.

3 Calculate the Solar Proton dose

This dose was calculated using the Solar Proton model JPL-91 and is statistical in nature. Consequently, it would not be valid to calculate the Solar Proton dose for one year, and scale up to a five year mission. Instead, the total Solar Proton dose over the five year period corresponding to 2004-2009 was calculated, a confidence level of 95% was used (which means that only 5% of possible missions would have a larger Solar proton dose).

4 Select the shielding values

A maximum shielding value of 20mm was used.

5 Calculate the ionising radiation dose for a given depth of Al shielding

The dose was calculated for both at the back of a finite Aluminium slab, and at the centre of an Aluminium sphere.

¹at www.spennis.oma.be/SPENVIS

6 Calculate the NIEL for a given depth of shielding

Results

The results for ionising radiation flux and proton flux assuming 3mm of Al are listed below, along with the two previous calculations (discussed in reference 1):

	SPENVIS	EEV analysis	J-side analysis
Ionising dose	1.6 krad/year	1.4 krad/year	1.8 krad/year
Non-ionising flux (10 Mev equivalent)	6.2×10^9 protons/cm ²	6×10^9 protons/cm ²	n/a

Figure one shows the variation in the proton flux >10MeV over the orbit (for 3mm Al shielding), and figure two shows the variation in the electron flux over the orbit. As can be seen, almost all of the proton flux occurs during passage through the SAA, and almost all of the electron flux occurs either through the SAA or in the Polar regions. For example, the total time spent in the SAA is about 13% of the orbit, but up to 95% of the proton flux occurs within just 5% of the orbit.

Figure three shows the variation in the trapped proton spectrum for values of Aluminium shielding thickness of 0.1 mm and 5mm. The lower energy protons, which contribute most to the ionising dose and NEIL, are substantially attenuated by only small amounts of shielding.

Variation in dark signal

The variation in the dark signal expected at the end of mission for different shielding thicknesses is shown in figures 4 and 5 for both MPP and non-MPP (non dithered). The proportional reduction in dark signal that can be achieved with increasing amounts of shielding decreases significantly for larger shielding thicknesses. Overall, it appears that the majority of any reduction in dark signal will be achieved by using an MPP device (or by using dithering) rather than small amounts of additional shielding.

Variation in ionising dose

The variation in yearly ionising dose with Al shielding thickness is shown in figure 6. From reference 2, the flat band voltage shift that can be expected is 50mV-120mV/krad. Thus, at the nominal shielding thickness of 3mm, a voltage shift of up to a volt could be expected. However, if 20mm of Al shielding was used, then a voltage shift of around 130mV is expected, which could be tolerated within the CCD operating tolerances and would not require additional software control of the CCD biases. (Nevertheless, it may still be preferable to include software voltage control unless such functionality is particularly complex).

The voltage shifts that could be expected over a five year mission for a range of shielding thicknesses is as follows:

Al thickness (mm)	dose (krad)/year	voltage shift (mV)
3	1.6	960

5	.74	440
10	.39	234
16	.27	162
20	.22	130

Transient events

To a first approximation, the energy deposited by an energetic proton will depend on the product of the ionising energy loss of the particle and its track length (reference 1). The higher the proton energy, the less will be the energy deposited in a single pixel. However, as one electron-hole pair will be created for every 3.6eV of energy deposited, it is clear that a high energy proton (several tens of MeV) can generate a substantial number of electrons within the area of a single pixel, and these electrons will be detected as transient, spurious charge when an image frame is processed.

There will be a large spread in the both the energies and the direction of arrival of the protons hitting the CCD. Consequently, it is not possible to specify the total number of pixels that will register the transient events unless a detailed mathematical model is used. For example, data from the Wide Field and Planetary Camera /2 CCD on Hubble suggests that on average, a single proton event effects six pixels. Lomheim et al. (1990, reference 3) measured the transient events for 17MeV protons at a range of angles and found that majority of protons incident at an angle of 70° to the front face of the CCD deposited energy in around 10-12 pixels. However, as such a calculation is very difficult, it has not currently been possible to estimate these effects and, in the calculations below, it has been assumed that one proton will cause transient charge to be deposited in only one pixel. To compare with the Hubble data, for example, the transient event rate calculated below should be multiplied by six.

The vast majority of the proton events will occur during passage through the SAA, with the majority of the electron events occur either during passage through the SAA, or during passage through the poles. For the purposes of this discussion, it has been assumed that the effect of protons on the transient event rate is much greater than the effect of electrons and gamma rays. This assumption is certainly valid at shielding values >5mm or so. For example, at 5mm the total dose contributed by electrons is an order of magnitude lower than the dose contribution from protons, and at 10mm the contribution is 3-4 orders of magnitude lower. For lower shielding depths the total dose contribution from the electrons approaches that of protons. However, as figures of LET have not been calculated for electrons, their effects have not been included in any calculation. Again, the calculated transient event rates for thicknesses of the order of 3mm or so should thus be seen as a minimum estimation.

For 3mm of Aluminium shielding, the overall proton flux is 6.2×10^9 protons/cm² over a five year period. The variation in proton flux during the 32 hour period was shown in figure 1. It can be seen that the proton flux varies, depending on the extent to which the orbit passes through the SAA. Figure 7 shows the orbit around period the 28 hour period in greater detail and shows how the overall proton flux will vary during a single passage. A proton flux of 6.2×10^9 protons/cm² corresponds to a flux of 4.2×10^6 protons/cm² over a 32 hour period. Given the flux distribution for this period shown in figure 1, the largest total flux that would be expected in the would be 8.5×10^5 protons/cm². Using the values in figure 7, the largest proton flux that would be expected (when passing through the centre of the SAA) would be 4500 protons/cm²/s.

Using the above calculation, the maximum transient event rate that could be expected for different shielding thicknesses is shown below:

thickness	proton flux over mission	max. transient event rate/cm ² /s	% of CCD/s
3mm	$6.2 \times 10^9 \text{ cm}^2$	4500	0.8
5mm	$4.5 \times 10^9 \text{ cm}^2$	3300	0.6
10mm	$3.6 \times 10^9 \text{ cm}^2$	2600	0.5
16mm	$2.9 \times 10^9 \text{ cm}^2$	2100	0.4
20mm	$2.6 \times 10^9 \text{ cm}^2$	394	0.3

The figures calculated above are larger than found with the WFPC/2 CCDs on board Hubble, but are not greatly larger. In addition, the inclination of Hubble (28° compared to 98° for Solar-B) means that it will receive a slightly smaller trapped proton flux, and will not encounter any solar protons from flares. Janesick et al. (1989, reference 4) estimated a proton flux passing through the SAA of about 2000 protons/cm²/s although this again was for a 30° inclination LEO orbit (and no values of shielding thickness were given). Overall, the calculated transient event rates are well within an order of magnitude agreement with other published data and should be seen as a reasonable estimation of the amount of reduction in the transient event rate that could be expected with additional shielding. It would be very useful to be able to compare the calculated rates above with those actually experienced on other space missions. TRACE is known to suffer from transient event problems both around the poles in and in the SAA (partly due to the low amount of shielding adopted). As TRACE has a similar LEO orbit to Solar-B, it is planned to use the TRACE data to obtain values of the transient event rate, and compare them to predictions from SPENVIS.

Should the final transient event rate be too high to allow imaging during these passes, a worst case option would be to switch off the CCD entirely for the time taken to pass through these areas. Around 95% of the total trapped proton flux occurs within 4% of the orbit, and this would be the period when measurements would not be possible should the transient event rate be too high. The transient event rate could be monitored in an area of the CCD, and as the whole of the CCD will not be used for the spectroscopic measurements, there will be several potential areas on the CCD which could be used to monitor the transient event rate. Until launch is completed, it will not be possible to specify exactly which areas of the CCD will be used to detect the spectroscopic image. Consequently, the ability to define a small area of the CCD, and constantly measure that area, would have to be selectable via software after launch.

Although it may be possible to reduce the number of transient events by adopting suitable shielding, there may still be enough of these events that the events will have to be removed in software. At the moment, it is planned that any removal of events will occur on the ground after compression has taken place rather than on-board.

It is not yet clear how the compression scheme adopted will be affected by the presence of very high frequency transient events. The J-PEG compression used for TRACE has experienced problems compressing these events, but it is believed that H-compress (likely to be used on EIS) does not suffer from so

many problems. Nevertheless, **it will be important to establish how effectively such transient events can be dealt with by the compression software.**

Once the data has been compressed and transmitted, there are a number of potential software methods that could be used to remove some of the transient events. For example, :

- Median filter - this technique is very simple, with each pixel replaced with the median value of the eight pixels surrounding it;
- Subtraction of images - The simple technique of subtracting two otherwise identical images is used on Hubble but it cannot be used to remove all of the image spikes as there is a small probability that some pixels will contain spikes in each image, which on Hubble is found to be about 4% of all pixels.

It is clear that a more detail study of the potential methods of removing transient images will need to be performed.

Charge Transfer Inefficiency

The effect of proton induced displacements on CTI is discussed in reference 2. The variation in CTI with shielding thickness in a particular CCD will be directly related to the variation in NIEL with shielding thickness. In turn, the variation in the NIEL will be directly related to the variation in the proton flux. This relationship was used to estimate the potential CTI in reference 2 and it was assumed that there was a linear relationship between the equivalent proton flux at 10MeV and the calculated CTI.

In reference 2, using a proton flux of 6×10^9 protons/cm², an approximate CTI at -50°C was calculated to be 0.00125, which corresponded to a 23% charge loss using an electron charge packet size of 1000.

The change in proton flux with shielding thickness is plotted in figure 8. The variation in the normalised CTI calculated above (i.e at 3mm) with shielding thickness is also plotted in figure 9. It is clear from figure 8, that a large proportion of the proton flux has already been stopped when 3mm of Aluminium shielding are used. This is to be expected, as the most damaging protons are at the lower end of the energy spectrum, and these are the ones most likely to be stopped with smaller amounts of shielding. The improvement gained in the CTI at 20mm shielding is not as great as would be hoped, but is still a halving of the CTI value for the nominal 3mm Aluminium shielding.

Overall, the reduction in CTI that can be expected for different thicknesses of shielding is tabulated below, using the CTI figure calculated in reference 2 of 0.00125 at -50°C:

Shielding thickness (mm)	CTI	% charge loss for 220 transfers
3	0.00125	23
7	0.00085	17
10	0.00074	15
16	0.00059	12
20	0.00053	11

The effect of different shielding for different sectors

Essentially, the EIS CCDs will be enclosed in a five sided Aluminium box, with the sixth side open to allow detection of spectra. The telescope itself has quite a large f-number, which means that little of the CCD front face could be enclosed by shielding near to the CCD itself.

Potentially, the lack of shielding around the front face of the CCD could lead to a large increase in both ionising dose and total proton flux, particularly the most harmful lower energy protons.

SPENVIS itself allows the effect of shielding to be calculated for three different geometries: the dose within a semi-infinite plane slab; the dose at the transmission side of a plane slab, infinite in the x and y directions; and the dose at the centre of an Aluminium sphere. However, it is not clear whether it is possible to make approximate sectoring calculations. A full sector analysis would be extremely complex, and is outside the scope of this work but it may be possible to estimate the increased dose and flux that could be expected due to the minimal shielding in the direction from the CCD front face. The CCD itself is not looking directly to space, and consequently will experience some protection from other spacecraft components. As can be seen from figures 3 and 8, even small amounts of shielding will remove many of the low energy contributions to both the dose and the proton flux.

Summary

Having calculated the variation in expected ionising radiation dose and proton flux, it is possible to make some general recommendations for the shielding that should be adopted for EIS:

1. the overall dark signal level is unlikely to be strongly effected by the shielding thickness chosen (providing a minimum shielding of 3mm at least is chosen). The choice of operating temperature and MPP/non-MPP operation are likely to have a much bigger effect;
2. with shielding of 15-20mm or so, the total ionising dose should be reduced sufficiently to remove the need to alter the CCD operating voltages during flight;
3. the peak transient event rate could be high, for example, with a 100 second integration, as much as 10% of the overall CCD may be affected by such events (with 3mm shielding). Adopting additional shielding does help, using 20mm thickness of shielding could reduce the events by as much as three times;
4. whilst the "baseline" shielding figure of 3mm should be sufficient to remove many of the low energy protons and electrons, ideally, as much shielding as is practical (for weight and space limits) is desirable to minimise the possible radiation effects. However, as the effect of additional shielding decreases for larger amounts of shielding it may be more effective to use smaller amounts. The thicknesses of shielding used in this study will not be sufficient to completely remove the undesirable effects of radiation. The maximum shielding thickness studied was 20mm which was sufficient to cut the possible CTI by half. Although this figure is not sufficient to remove any CTI problem completely (if there is found to be one) it should be sufficient to mitigate the effects somewhat. Given that only a few percent charge loss per frame transfer may degrade the image quality, it is probably best to aim for 20mm of shielding rather than (say) 15mm of shielding if at all possible. The current analysis does not include the additional radiation dose that will arise from those areas of the CCD

which are not protected by the dedicated shielding (for example, the front face of the CCD). However, it can be seen that even a small amount of shielding (3mm or so equivalent of Aluminium) will reduce the potential radiation dose and proton flux by several orders of magnitude.

Recommendations

The following recommendations arise out of this study:

- to minimise the effect of CTI and transient event, as large a shielding figure as is practical should be used. Ideally, this would be about 20mm or so of Aluminium, although 15mm of Aluminium shielding should be sufficient to significantly reduce these effects;
- any small amounts of additional shielding that can be added to the front sector of the CCD will have a substantial effect in reducing the radiation dose and proton flux in that area;
- as a full sector analysis has not been done (due to the complexity of such a study) it may be advisable to do so. The possibility has arisen of performing a full sector analysis using an "ideas" generated camera head design. It is recommended that we consider doing such an analysis once a stable design has been reached;
- TRACE data should be analysed to see how well the predicted transient events agree with actual events measured by TRACE. In addition, different potential software methods of removing the transient event "spikes" need to be investigated, along with the possible effects of using compression on the raw CCD data.

References

1. Radiation shielding Considerations for the Solar-B EIS CCDs - Initial Discussion. EIS-CCD-desnote-003
2. Radiation Concerns for the Operating Temperature Ranges for the EIS CCDs - Initial Discussion. EIS-CCD-desnote-002.
3. Hopkinson, G. R. "Proton Effects in Charge Coupled Devices". IEEE Transactions on Nuclear Science, Vol 43, No. 2. April 1996
- 4.
5. Janesick J., Elliot T., and Pool F. Radiation Damage in Scientific Charge Coupled Devices. IEEE Transactions on Nuclear Science, vol 36, No. 1 February 1989.

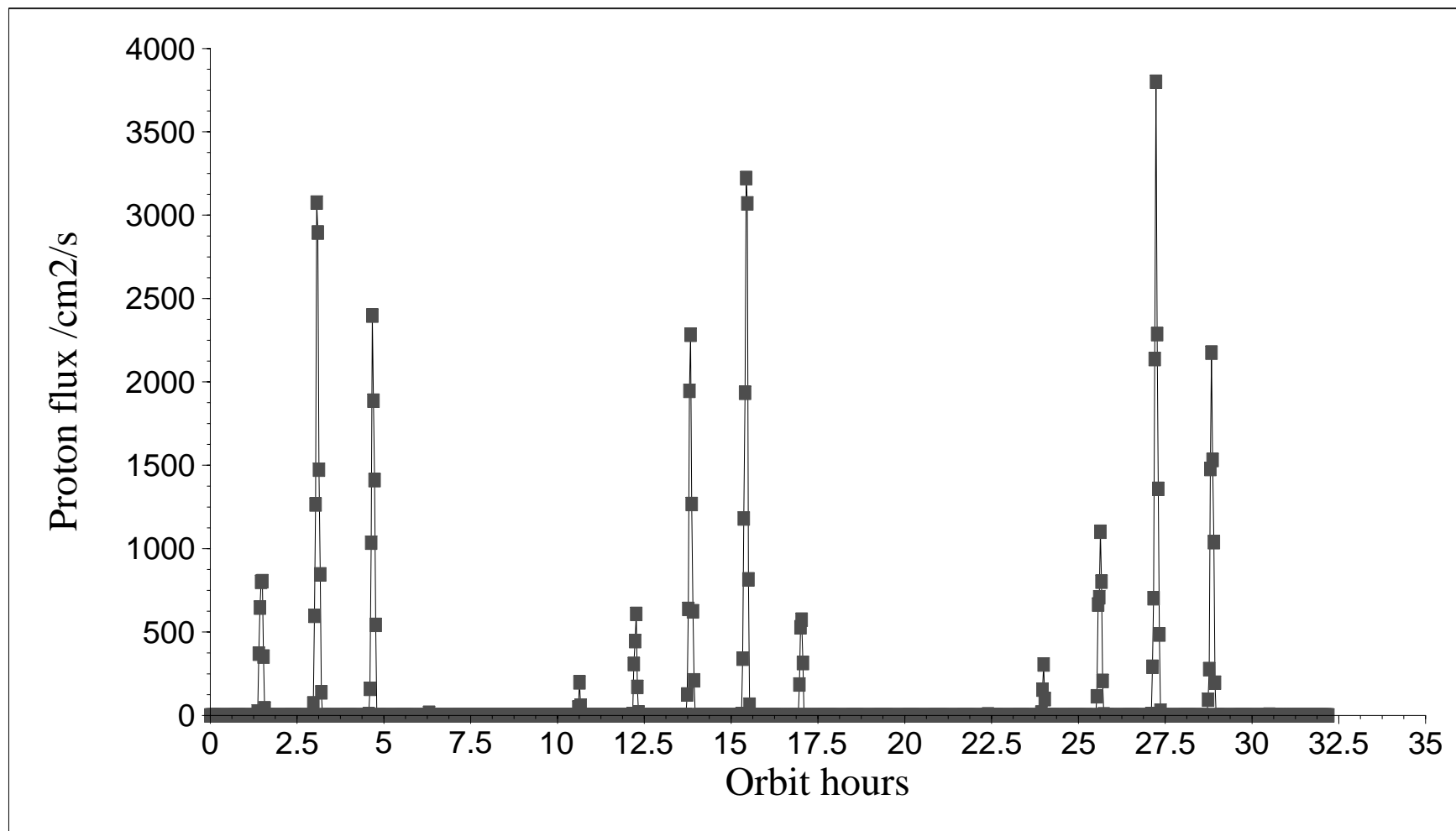


Figure 1: The variation in proton flux over an orbital period

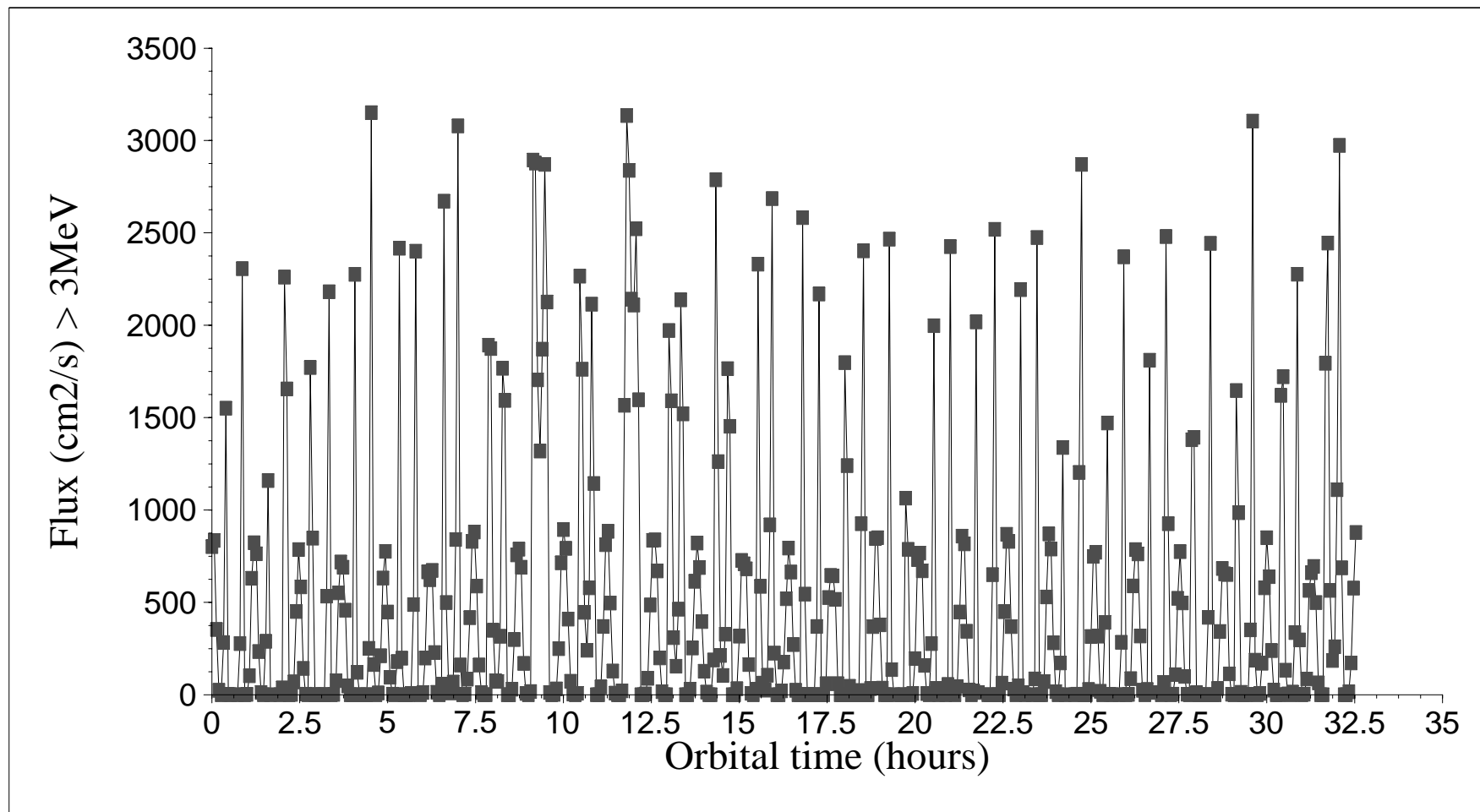


Figure 2: the electron flux > 3MeV

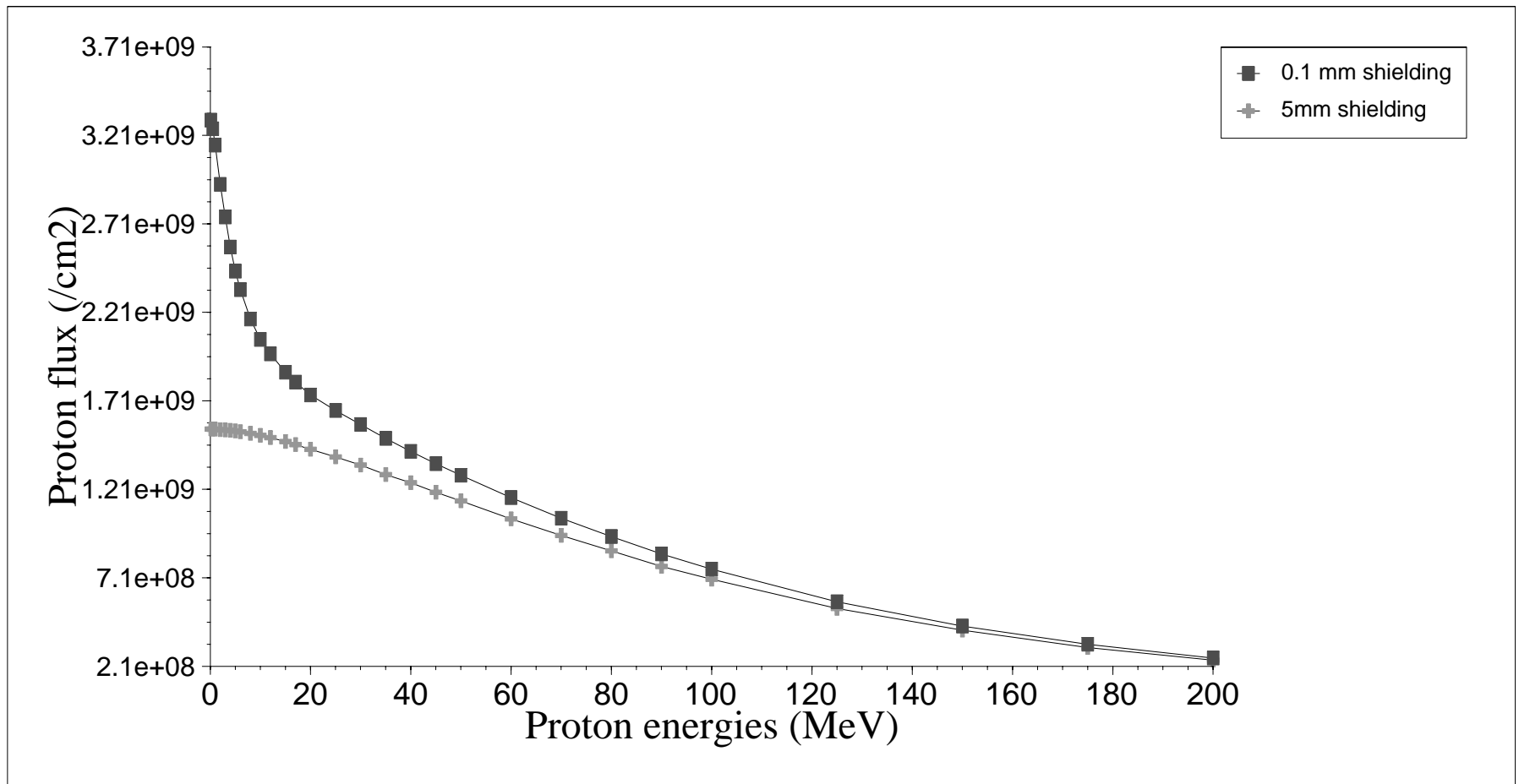


Figure 3: the trapped proton spectrum for two different shielding thicknesses

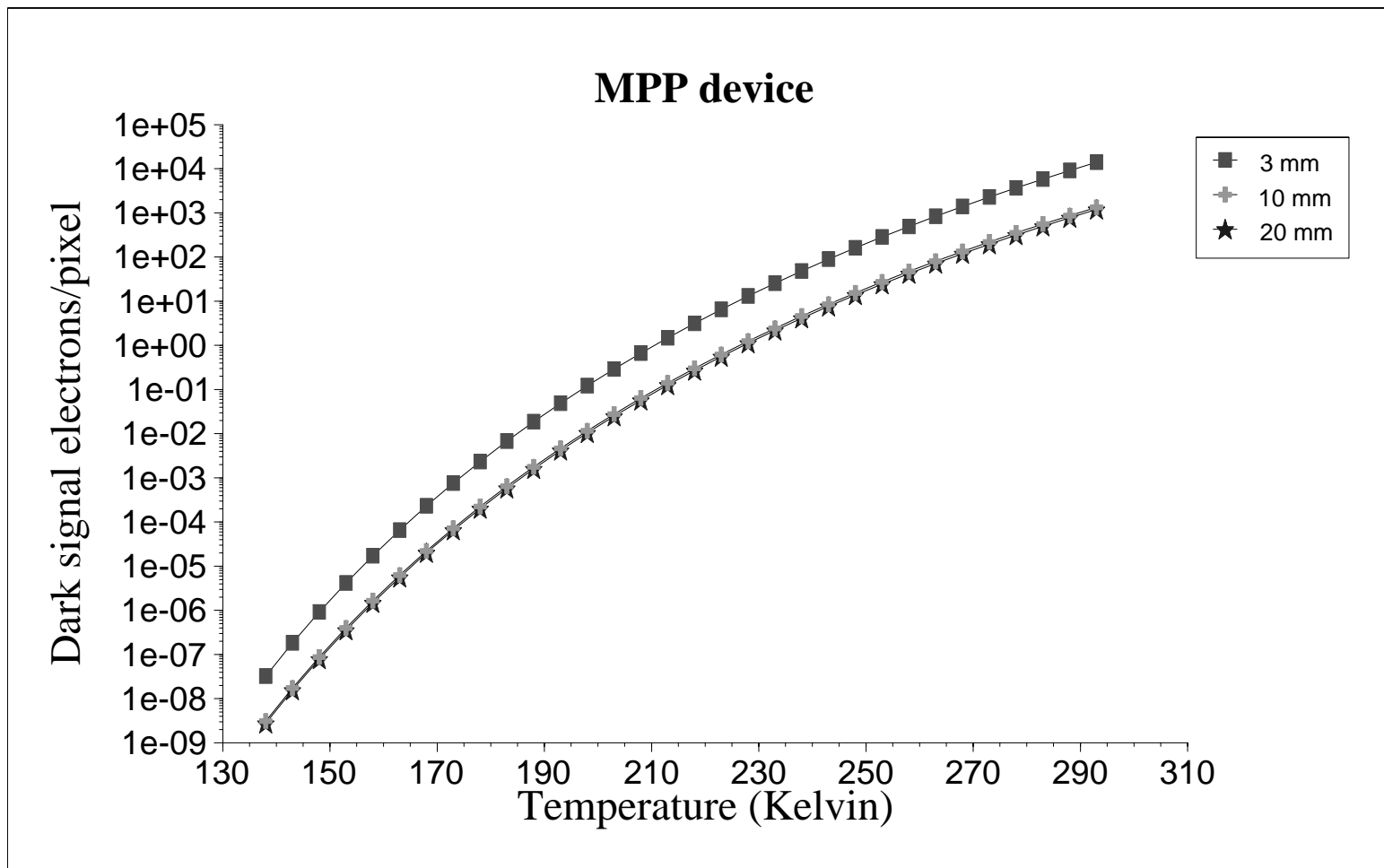


Figure 4: the variation in dark signal with shielding for an MPP device

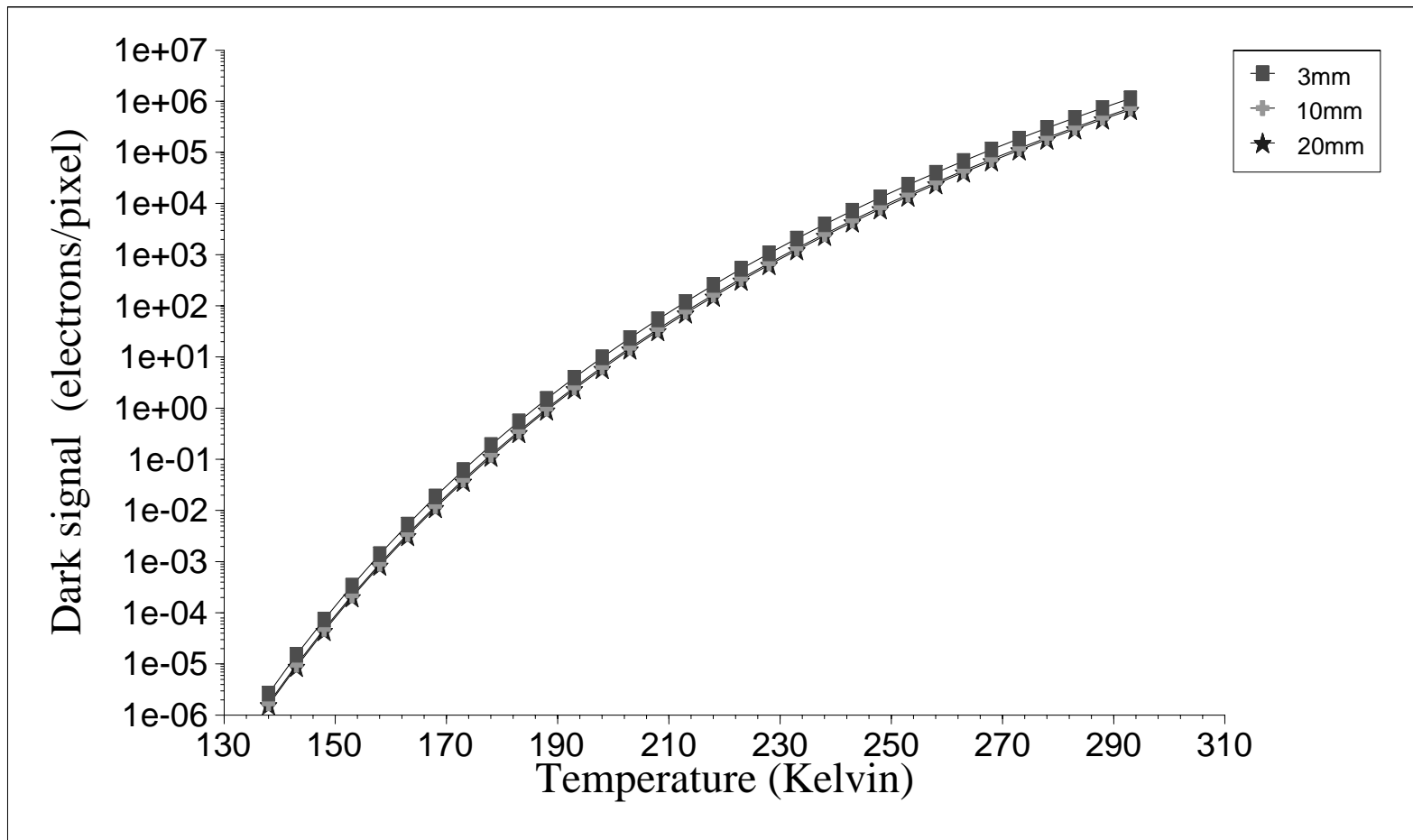


Figure 5: the variation in dark signal with shielding for a non MPP device

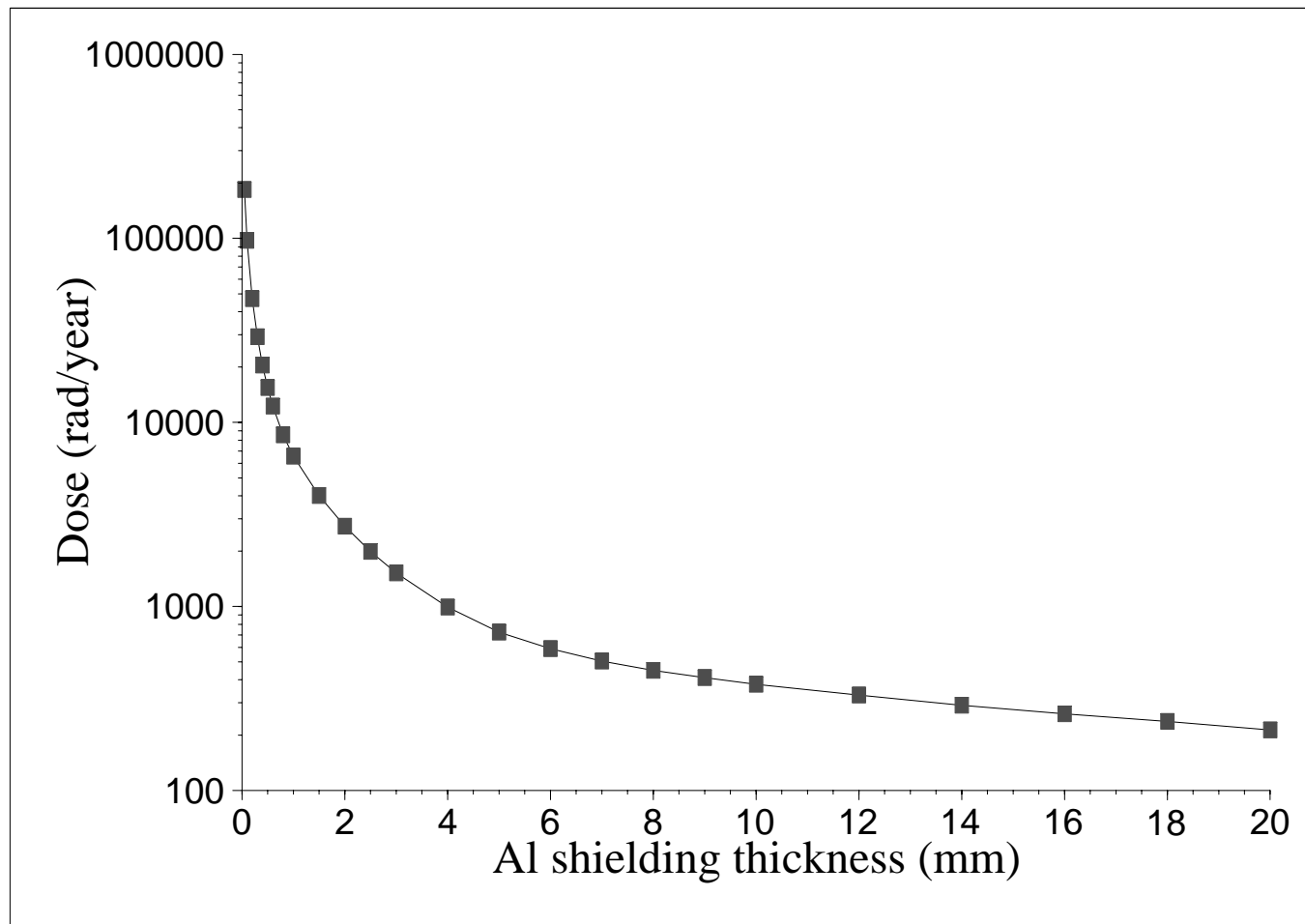


Figure 6: the variation in ionising dose rate for various shielding thicknesses

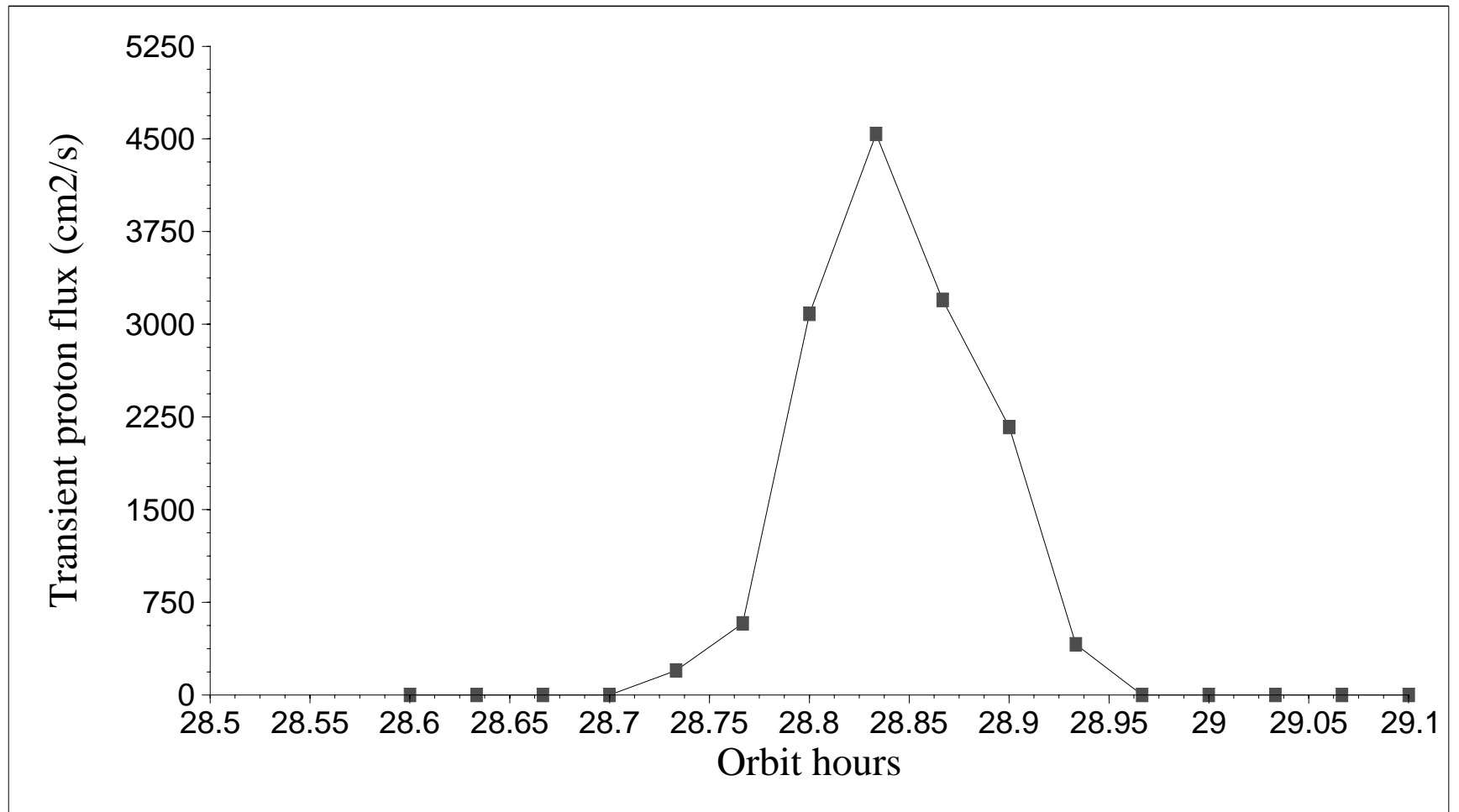


Figure 7: the variation in proton flux for one pass through the SAA

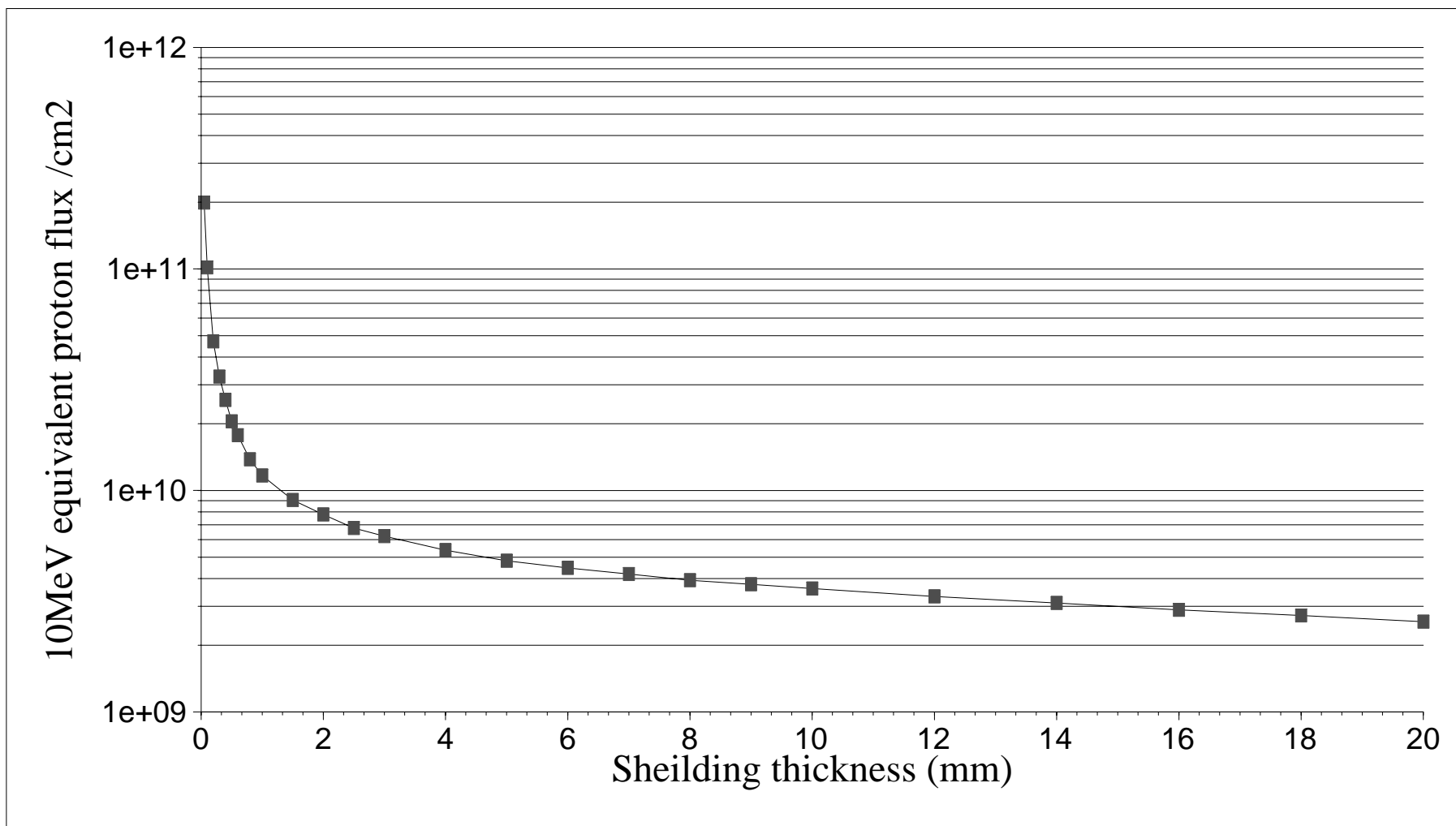


Figure 8: Variation in 10 MeV equivalent proton flux with shielding thickness

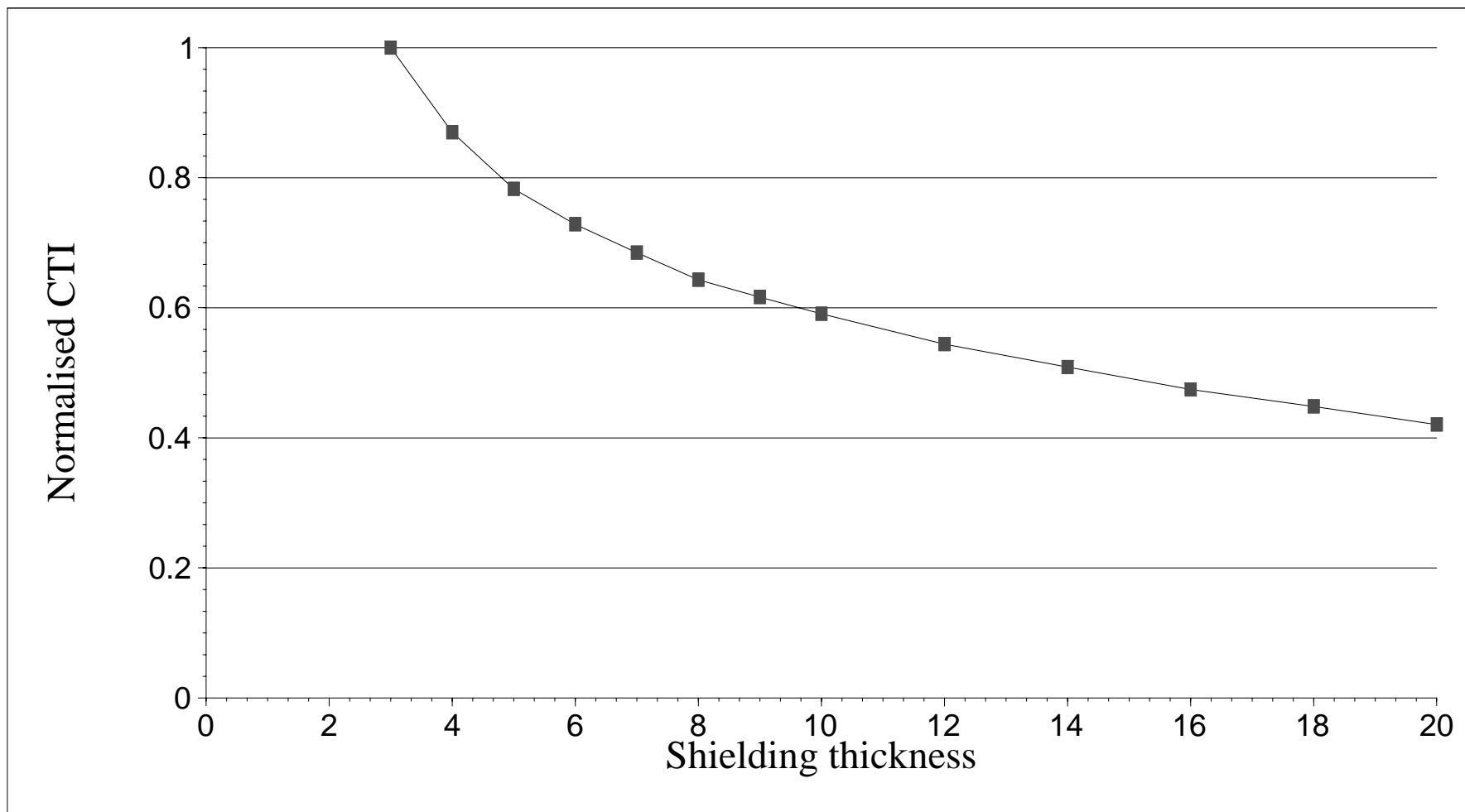


Figure 9: the variation in normalised CTI with shielding thickness